



This discussion paper is/has been under review for the journal Atmospheric Chemistry and Physics (ACP). Please refer to the corresponding final paper in ACP if available.

Comparison of surface and column measurements of aerosol scattering properties over the western North Atlantic Ocean at Bermuda

R. P. Aryal^{1,*}, K. J. Voss¹, P. A. Terman^{1,**}, W. C. Keene², J. L. Moody²,
E. J. Welton³, and B. N. Holben⁴

¹Department of Physics, University of Miami, Miami, FL 33146, USA

²Department of Environmental Sciences, University of Virginia, Charlottesville, VA 22904, USA

³Code 613.1, NASA GSFC, Greenbelt, MD, 20771, USA

⁴Code 614.4, NASA GSFC, Greenbelt, MD, 20771, USA

* now at: Department of Physics, Eckerd College, St. Petersburg, FL 33711, USA

** now at: Department of Physics and Astronomy, Texas A&M University, College Station, TX 77843, USA

Received: 23 August 2013 – Accepted: 8 January 2014 – Published: 21 January 2014

Correspondence to: K. J. Voss (voss@physics.miami.edu)

Published by Copernicus Publications on behalf of the European Geosciences Union.

Comparison of surface and column measurements of aerosol scattering

R. P. Aryal et al.

Title Page

Abstract

Introduction

Conclusions

References

Tables

Figures



Back

Close

Full Screen / Esc

Printer-friendly Version

Interactive Discussion



atmospheric aerosols represent a major constraint in our ability to predict Earth's climate (IPCC, 2007).

Detailed measurements of near-surface aerosol characteristics provide important constraints in developing reliable retrieval algorithms for remotely sensed parameters.

5 More generally, synchronized measurements from ground- and satellite-based platforms facilitate more reliable spatial and temporal extrapolation of the chemical, physical, and optical properties of aerosols and their associated climatic implications (Russel et al., 2000; Bates et al., 2006). For logistical reasons, long-term measurement campaigns of aerosol physiochemical properties are typically limited to surface sites.

10 These measurements are often assumed to be representative of the overlying aerosol column, or at least of the aerosol boundary layer. Paired measurements of optical properties through the column allow this assumption to be evaluated explicitly (Voss et al., 2001a).

15 In this study the optical and physical characteristics of aerosols were measured simultaneously in near-surface air and in the overlying column at Bermuda during winter and spring 2009. Paired data ensembles are compared to evaluate the representativeness of near-surface optical properties for the overlying column.

2 Methods

2.1 Site description and sampling strategy

20 Bermuda (32.24° N, 64.87° W) is influenced by the long-range transport of chemically and optically distinct air masses originating from different source regions, the relative importance of which vary seasonally (Galloway et al., 1989; Moody et al., 1995, 2013; Anderson et al., 1996). Westerly flow, which is most frequent during winter and spring, transports emission products from North America, over the western North Atlantic, to the island. Southerly and southeasterly flow, which is most prevalent during summer, transports Saharan dust intermixed with emission products from Europe and Africa to

Comparison of surface and column measurements of aerosol scattering

R. P. Aryal et al.

Title Page

Abstract

Introduction

Conclusions

References

Tables

Figures



Back

Close

Full Screen / Esc

Printer-friendly Version

Interactive Discussion



Comparison of surface and column measurements of aerosol scattering

R. P. Aryal et al.

Title Page

Abstract

Introduction

Conclusions

References

Tables

Figures

⏪

⏩

◀

▶

Back

Close

Full Screen / Esc

Printer-friendly Version

Interactive Discussion

via a laminar flow plenum. Air from the center of the plenum was drawn through an inlet heated to a temperature $28 \pm 5^\circ\text{C}$ to dehydrate aerosols prior to analysis, an inertial impactor to differentiate size fractions, and then the nephelometer. The switched impactor was configured with aerodynamic size cuts of 10.0 and 1.0 μm diameter to alternately characterize scattering by bulk and sub- μm diameter size fractions. Scattering by super- μm size fractions was calculated by difference (bulk minus sub- μm). Temperature and RH in the sampling chamber were monitored and recorded. The nephelometer was routinely calibrated with clean CO_2 (Anderson and Ogren, 1998). During each hour, clean particle-free air was introduced into the chamber to obtain a zero value for 20 min, scattering by bulk aerosol was measured for 20 min, and scattering by sub- μm aerosol was measured for 20 min.

The scattering coefficient (in Mm^{-1}) at 530 nm for each size fraction (sub- μm and bulk) in near surface air ($b_{\text{size-surf}}$) was calculated via

$$b_{\text{size-surf}} = \left| \frac{b_{\text{size-surf}} - b_{\text{zero}}}{b_{\text{cal}} - b_{\text{zero}}} \right| \cdot 20 \text{Mm}^{-1} \quad (1)$$

where $b_{\text{size-samp}}$ is scattering measured in ambient samples, b_{cal} is scattering by clean CO_2 , b_{zero} is scattering by particle free air. The scattering coefficient due to clean CO_2 is 20Mm^{-1} based on the average temperature $28 \pm 5^\circ\text{C}$ and pressure $995 \pm 11 \text{mb}$ (Anderson and Ogren, 1998). The scattering coefficients were then filtered to remove values outside the operating range specified by the manufacturer (1 to 1000Mm^{-1}). Values exceeding the upper limit typically reflected artifacts associated with overheating of the instrument. The continuous data set was then filtered to extract the subset of scattering data that corresponded to periods of no precipitation during which on-shore winds were from the open-ocean sector at velocities greater than 1ms^{-1} thereby minimizing local influences. The reported values of the scattering coefficient were adjusted to account for truncation error, which exist due to the internal geometry of the instrument that prevents measurement in the near forward and near backward scattering region. Anderson and Ogren (1998) showed that the nephelometer is sensitive to scat-

Comparison of surface and column measurements of aerosol scattering

R. P. Aryal et al.

Title Page

Abstract

Introduction

Conclusions

References

Tables

Figures

◀

▶

◀

▶

Back

Close

Full Screen / Esc

Printer-friendly Version

Interactive Discussion



tering of light in the angular range of $\sim 7^\circ$ – 170° . The truncation error is present both during calibration of the nephelometer and during measurement of aerosol light scattering. In this text we have used an average correction factor for scattering by sub- μm and bulk aerosols, 1.08 ± 0.004 and 1.18 ± 0.04 respectively, which were determined based on calculations from Mie theory. The input parameters, aerosol volume size distribution, and index of refraction were obtained from AERONET inversions (Holben et al., 1988) for the Bermuda site (e.g. see Sect. 2.3.1). The relative contribution of particle free air to this correction factor was calculated using a Rayleigh scattering phase function (Ensor et al., 1970).

Note that aerosol absorption was also measured at the site, using a filter reflectance technique (Aryal et al., 2014), but this measurement will not be used in the present paper because there was no corresponding column measurement with which to compare.

2.3 Measurements and calculated characteristics of the atmospheric column

2.3.1 Sun and sky radiometer

An automated CIMEL sun and sky radiometer was deployed at the top of the tower in December 2007 as a part of AERONET (Aerosol Robotic Network). Numerous publications describe the instrumentation, data acquisition, retrieval algorithm, calibration procedures, cloud-screening procedures as well as the uncertainty of the final products (Holben et al., 1998; Smirnov et al., 2000). Direct solar irradiance is measured at eight spectral channels 340, 380, 440, 500, 675, 870, and 1020 nm and used to compute the aerosol optical depth (AOD, τ). Direct solar irradiance at 940 nm is used to retrieve precipitable water vapor. The uncertainty in retrieval of τ under cloud free conditions is $< \pm 0.01$ for $\lambda > 440$ nm and $< \pm 0.02$ for shorter wavelengths (Holben et al., 1998; Eck et al., 1999).

In addition, sky radiance was measured at 440, 670, 870, and 1020 nm through a large range of scattering angles from the sun several times in the day. The sky

Comparison of surface and column measurements of aerosol scattering

R. P. Aryal et al.

Title Page

Abstract

Introduction

Conclusions

References

Tables

Figures

◀

▶

◀

▶

Back

Close

Full Screen / Esc

Printer-friendly Version

Interactive Discussion

radiance and direct solar irradiance were used, assuming a constant aerosol profile, to retrieve the column averaged size distribution and the spectral refractive index. AERONET provides inversion products for three data quality levels: level 1.0 (unscreened), level 1.5 (automatically cloud screened) following the methodology as described by A. Smirnov et al. (2000), and level 2 (cloud screened and quality assured). The analysis reported here is based on level 2 products.

Dubovick et al. (2000) investigated the accuracy of the AERONET inversion products and found that while the size distribution of the aerosols could be resolved reliably at all aerosol optical depths, the inversion for the complex index of refraction was sensitive to this factor. The real portion of the index of refraction had an uncertainty of 0.05 for $\tau_{440} < 0.2$, and the imaginary part had an uncertainty of 80–100 % for these low values. The complex index of refraction was reliably retrieved for $\tau_{440} > 0.4$. In the data set used in this paper we had no cases with $\tau_{440} > 0.4$, and only one case with $\tau_{440} > 0.2$. We had to use the complex index of refraction resulting from the inversion in our Mie calculations, described below, and accept that the uncertainty in this value could be large. Because the imaginary part of the index of refraction determines the absorption of the aerosol, and was highly uncertain, thus there was no accurate derived column absorption property with which to compare the surface values.

2.3.2 Micro-pulse lidar

A Micro-pulse lidar (MPL, Spinhirne et al., 1995) was installed at the base of the tower in March 2008 and operated continuously during the measurement period as part of NASA's MPL Network (MPLNET, Welton et al., 2001). The MPL system employs an optical transceiver that acts as both transmitter and receiver (telescope) and consists of a diode pumped ND : YLF (neodymium-doped YLF, acronym for yttrium lithium fluoride) laser at 527 nm, an Single Photon Counting Module (SPCM) Avalanche Photo Diode (APD) detector, a signal processing unit, and data processor. MPLNET level 1 signal profiles and associated uncertainties (Campbell et al., 2002; Welton et al., 2002) are generated continuously, at 75 m vertical and 1 min time resolutions. Profiles of aerosol

The columnar size distribution can be rewritten in terms of the volume size distribution as:

$$n_c(d) = \frac{6}{\pi d^4} \cdot \frac{dV(d)}{d \ln d} \quad (3)$$

The temporal complex refractive indices at 530 nm were obtained by interpolating corresponding temporal spectral AERONET inversion data between the spectral refractive index data at 438 nm and 675 nm by assuming that the aerosol refractive index is a weak function of the wavelength in this range of wavelength. The AERONET inversion gave the volume size distribution ($dV(d)/d \ln d$) at 22 logarithmically equidistant points in the size range $0.1 \mu\text{m} \leq d \leq 30 \mu\text{m}$ (Dubovik and King, 2000). These ambient volume size distributions were interpolated at $0.004 \mu\text{m}$ diameter steps in the two different size ranges of $d < 1 \mu\text{m}$ and $< 10 \mu\text{m}$ for quantitative comparison with the near surface sub and bulk- μm dehydrated aerosol data.

2.3.4 Radiosonde measurements

Radiosonde measurements were performed twice daily during our measurement period at the L. F. Wade International Airport by the Bermuda Weather Service. Data for our measurement period was downloaded from the NOAA Integrated Global Radiosonde Archive (IGRA). The radiosonde temperature data below 1 km (typically only 2–3 data points) was used to calculate a lapse rate (Calvert, 1990) for the lower atmosphere, which can be used as an indication of the stability of the atmosphere. The average atmospheric lapse rate is $-6.5^\circ\text{C km}^{-1}$, values less than this indicate a stable atmosphere, less likely to be well mixed, while values above indicate an unstable atmosphere, and more likely to be well mixed (Calvert, 1990). We also used the dew point temperature depression to calculate the relative humidity (Lawrence, 2005) and interpolate this parameter to the altitude of the lowest MPL extinction measurement (400 m).

Comparison of surface and column measurements of aerosol scattering

R. P. Aryal et al.

Title Page

Abstract

Introduction

Conclusions

References

Tables

Figures

⏪

⏩

◀

▶

Back

Close

Full Screen / Esc

Printer-friendly Version

Interactive Discussion



2.3.5 Flow regime analysis

To see if the emission source influenced the column/surface relationships the data set was classified by transport pattern. A particle dispersion model, FLEXPART (Stohl et al., 1998, 2005) was run in back trajectory mode (Stohl et al., 2003; Siebert and Frank, 2004). The FLEXPART trajectories were classified into 5 groups depending on fractional footprint residence times. These groups were northeastern United States (NEUS), southeastern United States and the Gulf of Mexico (East-SEUS), Northern Africa and the eastern tropical Atlantic (Africa), Ocean – when the transport resulted in long residence times over the open ocean, and North – a combination of North Atlantic and northeastern United States. More details on this breakdown are provided in Moody et al. (2013).

3 Results and discussions

3.1 Column AOD and scattering coefficient for bulk aerosol in sectored near-surface air

Extinction is typically dominated by scattering (Kokanovsky, 2008). Consequently, if the optical properties and quantities of aerosols near the surface are representative of those in the overlying column, τ and the scattering coefficient for bulk aerosol ($b_{\text{bulk-surf}}$) near the surface should be correlated. To obtain coincident data sets, and avoid problems due to temporal variability of meteorological conditions (such as wind speed, relative humidity), origins and paths of air masses (Calvello et al., 2010), we report column aerosol data that correspond to the periods of near-surface measurements. The paired hourly averaged data (AOD at 500 nm (τ_{500}) and $b_{\text{bulk-surf}}$) correspond to those having a minimum of three AOD measurements.

Time series τ_{500} , and $b_{\text{bulk-surf}}$ are generally correlated (Fig. 1); deviations reflect the influence of the variability in the vertical structure of the distribution of aerosol mass,

Comparison of surface and column measurements of aerosol scattering

R. P. Aryal et al.

Title Page

Abstract

Introduction

Conclusions

References

Tables

Figures



Back

Close

Full Screen / Esc

Printer-friendly Version

Interactive Discussion



size distributions, morphology, and composition within the column (Bergin et al., 2000; Voss et al., 2001a). For example, vertical profiles of aerosol extinction from MPLNET on 23 March 2009 at 13:42 and 13:57 UTC (DOY 82), which are marked by A in Fig. 1a are shown in Fig. 2. They have an average τ_{500} but remarkably low $b_{\text{bulk-surf}}$ relative to the corresponding values for entire study period. It is evident from Fig. 2 that the enhanced extinction associated with an elevated aerosol layer at approximately 1.8 km is responsible for a high τ_{500} relative to $b_{\text{bulk-surf}}$.

Moody et al. (2013) describe variability in aerosol characteristics as a function of atmospheric flow regime over the 3 yr period from July 2006 through June 2009. Over the 6 month period of this study there does not seem to be a clear grouping of the measured surface $b_{\text{bulk-surf}}$, nor τ by flow regime. Nor is there a clear over- or underestimate of the column τ_{500} , given the surface $b_{\text{bulk-surf}}$, in specific regimes (Fig. 1b). The fit of τ_{440} was used to generate an error factor, which indicated how poorly the surface value was correlated with the column measurement. This was then plotted against the lower atmosphere's (less than 1 km) environmental lapse rate, as shown in Fig. 1c. There does not seem to be a dependence on either flow regime or error in prediction with lapse rate, other than the data point with the largest error did occur at a time with a low lapse rate, hence stable and possibly unmixed atmosphere. There were only two radiosonde measurements/day, and the one nearest to the optical measurement was used, however there could be time difference between the two measurements of up to 6 h.

Monthly averages for the paired data subsets are reported in Table 1. For the entire analysis period, the mean $\tau_{500} \pm \sigma$ was 0.12 ± 0.03 and the range was 0.06 ± 0.01 to 0.22 ± 0.01 . The average value of τ_{500} was statistically indistinguishable from the global averaged oceanic AOD (~ 0.11) reported by Smirnov et al. (2009). The mean near-surface scattering coefficient, $b_{\text{bulk-surf}}$ was $13.52 \pm 6.32 \text{ Mm}^{-1}$ and the corresponding range was 2.78 ± 0.41 to $32.25 \pm 0.64 \text{ Mm}^{-1}$. The minimum values for τ_{500} and $b_{\text{bulk-surf}}$ were observed at the same times as were the maximum values. In Fig. 3, the vertical aerosol extinction profile obtained from MPLNET is shown. It is evident that in this

Comparison of surface and column measurements of aerosol scattering

R. P. Aryal et al.

Title Page

Abstract

Introduction

Conclusions

References

Tables

Figures



Back

Close

Full Screen / Esc

Printer-friendly Version

Interactive Discussion

case, the higher aerosol concentrations below 1 km are primarily responsible for higher column AOD, τ_{500} .

3.2 Sub- μm scattering fraction for sectored near-surface data and column-averaged extinction Angstrom exponent (α)

5 The sub- μm scattering fraction ($R_{\text{sub-surf}}$) for the aerosol population is the ratio of the scattering coefficient for the sub- μm -diameter size fraction to the scattering coefficient for bulk aerosol (i.e., $b_{\text{sub-surf}}/b_{\text{bulk-surf}}$) and, thus, provides an indication of the relative contribution of small particles to total scattering.

10 The extinction Angstrom exponent (α) was calculated from the spectral AOD using the following formula:

$$\alpha = -\log\left(\frac{\tau_1}{\tau_2}\right) / \log\left(\frac{\lambda_1}{\lambda_2}\right) \quad (4)$$

15 Where τ_1 and τ_2 are column AOD at corresponding wavelengths λ_1 and λ_2 . When α is computed over a sufficiently large wavelength interval, including both the visible (440 nm) and near infrared (870 nm), it is sensitive to the relative contributions of fine and coarse mode particles; α increases with decreasing particle size (Schuster et al., 2006). When α is less than 1, extinction is dominated by super- μm diameter particles and when greater than 1 extinction is dominated by sub- μm diameter particles (Eck et al., 1999; Reid et al., 1998). A scatter plot of the hourly average α calculated from the instantaneous spectral AODs from AERONET at 400 nm and 870 nm vs. $R_{\text{sub-surf}}$ based on the hourly averaged near-surface sectored air is shown in Fig. 4. The correlation coefficient (0.72) between α and $R_{\text{sub-surf}}$ indicates that the relative variability in the extinction associated with the column-averaged size distribution is similar to that associated with aerosols near the surface. Relative to sub- μm aerosol size fractions, super- μm size fractions are associated with greater dry-deposition velocities and consequently, on average, their concentrations decrease more rapidly with altitude (e.g., Lewis and Schwartz, 2006). Variability in vertical gradients of the size distribution as

Comparison of surface and column measurements of aerosol scattering

R. P. Aryal et al.

Title Page

Abstract

Introduction

Conclusions

References

Tables

Figures

⏪

⏩

◀

▶

Back

Close

Full Screen / Esc

Printer-friendly Version

Interactive Discussion



a function of wind velocity and other factors contribute to variability around the regression line of Fig. 4.

As one would expect, the extinction Angstrom exponent varies as a function of flow regime. Low Angstrom exponents were a characteristic of the North flow (median was 0.054, with a standard deviation of 0.18). For the other flow regimes, the Angstrom exponents were generally 0.9–1.0 with standard deviations of 0.24–0.32, thus not distinguishable. An analysis of the difference between the predicted Angstrom exponent, based on $R_{\text{sub-surf}}$, and lapse rate did not show a relationship, as with Fig. 1c. In general though, there was a correlation between the magnitude of the error in predicted AOD and the error in the magnitude of predicted extinction Angstrom exponent. In other words, if the surface measurement was not correlated well with the column measurement for one parameter, it was also true for the other.

3.3 Sub- μm scattering fraction of light in sectored near-surface air and the column average

We also compared the sub- μm scattering fraction ($R_{\text{sub-col}}$) determined with Mie calculations using the column-averaged parameters (size distribution and index of refraction) with the near-surface sub- μm scattering fraction ($R_{\text{sub-surf}}$) based on hourly averages (Fig. 5). Results reveal a significant linear correlation. However, the surface values were typically less than the corresponding column values and relative differences were greater at lower surface $R_{\text{sub-surf}}$. This result indicates that scattering by the super- μm size fraction was greater near the surface relative to the column, which is consistent with expectations based on the relatively greater concentrations of super- μm diameter marine aerosol in near-surface air. We also found a dependence in relative variability as a function of wind speed (Fig. 6), $R_{\text{sub-col}}$, and $R_{\text{sub-surf}}$ are inversely correlated with wind speed and the slope is steeper for near-surface aerosol relative to the column average.

Kleefeld et al. (2002) report similar relationships. These results reflect the greater production fluxes, and higher concentrations of super- μm marine aerosols at higher

Comparison of surface and column measurements of aerosol scattering

R. P. Aryal et al.

Title Page

Abstract

Introduction

Conclusions

References

Tables

Figures

⏪

⏩

◀

▶

Back

Close

Full Screen / Esc

Printer-friendly Version

Interactive Discussion



wind speeds, along with stronger vertical gradients in aerosol mass, and associated influences on light scattering by super- μm aerosol size fractions.

3.4 Comparison of surface level aerosol scattering data and extinction coefficient derived from lidar measurements

We compared the scattering coefficient for near-surface aerosol measured with the nephelometer with the corresponding extinction coefficient ($C_{\text{ext},527}$) obtained at the lowest altitude bin (400 m) from the lidar inversion (Welton, 1998; Voss et al., 2001a). Direct comparison is complicated by the fact that these measurements were at different relative humidities and temperatures and correspond to slightly different altitudes. In particular, the lidar characterized scattering by hydrated aerosols at ambient relative humidity whereas the nephelometer characterized dry aerosols, thus differences are expected (Zieger et al., 2011). The impact of hygroscopic growth on the aerosol light scattering coefficient is usually described by the scattering enhancement factor, f (RH), at a given wavelength, λ , which is defined as

$$f(\text{RH}) = b_{\text{bulk-surf}}(\text{RH})/b_{\text{bulk-surf}}(\text{RH}_{\text{dry}}) \quad (5)$$

The scattering coefficient is typically measured with dry particles when $\text{RH} < 30\text{--}40\%$ (WMO/GAW, 2003). Modeled and measured scattering enhancement factors ($f(\text{RH})$) have been described for different types of aerosols such as maritime (Carrico et al., 1998, 2003; Wang et al., 2007), urban (Yan et al., 2009), continental (Sheridan et al., 2001), biomass burning (Kotchenruther and Hobbs, 1998), and free tropospheric aerosol (Fierz-Schmidhauser et al., 2010). At an ambient RH of 80%, $f(\text{RH})$ for sea salt aerosol ranges from 1.8 to 3.2 (Lewis and Schwartz, 2004).

The retrieved lidar extinction coefficient at the lowest height bin and the $b_{\text{bulk-surf}}$ measured by the nephelometer are linearly correlated ($r = 0.77$) but the slope differs significantly from 1 (Fig. 7). The time series of the ratio of the extinction coefficient from the lidar data to the scattering coefficient from the nephelometer, $R_{\text{mpl/neph}}$, is shown in

Comparison of surface and column measurements of aerosol scattering

R. P. Aryal et al.

Title Page

Abstract

Introduction

Conclusions

References

Tables

Figures

⏪

⏩

◀

▶

Back

Close

Full Screen / Esc

Printer-friendly Version

Interactive Discussion



Fig. 8. The extinction coefficient retrieved at the lowest altitude bin (400 m) was about 3.4 ± 0.3 times greater than the scattering coefficient measured with the nephelometer.

As mentioned earlier, we can use radiosonde data to calculate the RH at the lowest altitude bin of the MPL (400 m). We calculated the RH and broke our data set into 5 % RH bins, to evaluate variation in the inferred $f(\text{RH})$ as a function of RH (Fig. 9) The average $R_{\text{mpl/neph}}$ exhibited little variability at RHs less than 70 %, increases between 70 % and 80 %, and decreased at higher RHs. However, the large standard deviations within each RH bin ($> \pm 1$) suggest that factors other than RH accounted for most of the variability. Others have found that this ratio increases with RH, highlighting the influence of RH on aerosol light scattering (Zieger et al., 2011). With a larger data set it might be possible to eliminate the confounding issues of aerosol type to investigate the $f(\text{RH})$.

4 Conclusions

Using a suite of instruments operating in parallel (including a Nephelometer; Cimel Sun-photometer, MPL) we simultaneously quantified several aerosol optical properties in near-surface air and in the overlying column at Bermuda from January 2009 to June 2009. In most cases, optical properties near the surface were highly correlated with those in the column. When surface properties diverged significantly from the column integrated values, vertical lidar profile often revealed vertical structure that accounted for differences.

At the higher windspeeds, enhanced production of marine aerosols sustain relatively higher concentrations of super- μm -diameter size fractions in near-surface air that resulted in systematic divergence between the column vs. near-surface sub- μm scattering fraction. The generally good agreement between the paired measurements suggest that, in most cases, aerosol optical properties measured at the surface can be extrapolated with reasonable confidence to the overlying atmosphere.

Comparison of surface and column measurements of aerosol scattering

R. P. Aryal et al.

Title Page

Abstract

Introduction

Conclusions

References

Tables

Figures



Back

Close

Full Screen / Esc

Printer-friendly Version

Interactive Discussion



Comparison of surface and column measurements of aerosol scattering

R. P. Aryal et al.

Title Page

Abstract

Introduction

Conclusions

References

Tables

Figures

⏪

⏩

◀

▶

Back

Close

Full Screen / Esc

Printer-friendly Version

Interactive Discussion

Acknowledgements. We thank Miguel Izaguirre, Kim Zeeh and Chris Marsay for assisting in field operations and data generation and processing. Peter Sedwick and Andrew Peters supervised operations at the observatory and the Bermuda Institute for Ocean Sciences provided outstanding logistical support. Funding was provided by the National Science Foundation through awards to the University of Miami (ATM 0541 566) and the University of Virginia (ATM 0541 570). Additional support was provided by NASA through the AERONET and MPLNET programs. MPLNET is supported by the NASA Radiation Sciences Program and NASA Earth Observing System.

References

- Anderson, J. R., Buseck, P. R., Patterson, T. L., Arimoto, R.: Characterization of the Bermuda Troposphere Aerosol by combined individual particle and bulk aerosol analysis, *Atmos. Environ.*, 30, 319–338, 1996.
- Anderson, T. L. and Ogren, J. A.: Determining aerosol radiative properties using the TSI 3563 integrating nephelometer, *Aerosol Sci. Tech.*, 29, 57–69, 1998.
- Aryal, R., Terman, P., and Voss, K. J.: Comparison of two filter-based reflectance methods to measure the light absorption by atmospheric aerosols, *J. Atmosph. Ocean. Tech.*, accepted, 2014.
- Bates, T. S., Anderson, T. L., Baynard, T., Bond, T., Boucher, O., Carmichael, G., Clarke, A., Erlick, C., Guo, H., Horowitz, L., Howell, S., Kulkarni, S., Maring, H., McComiskey, A., Middlebrook, A., Noone, K., O'Dowd, C. D., Ogren, J., Penner, J., Quinn, P. K., Ravishankara, A. R., Savoie, D. L., Schwartz, S. E., Shinozuka, Y., Tang, Y., Weber, R. J., and Wu, Y.: Aerosol direct radiative effects over the northwest Atlantic, northwest Pacific, and North Indian Oceans: estimates based on in-situ chemical and optical measurements and chemical transport modeling, *Atmos. Chem. Phys.*, 6, 1657–1732, doi:10.5194/acp-6-1657-2006, 2006.
- Bergin, M. H., Schwartz, S. E., Halthore, R. N., Ogren, J. A., and Hlavka, D. L.: Comparison of aerosol optical depth inferred from surface measurements with that determined by sun photometry for cloud free conditions at a continental US site, *J. Geophys. Res.*, 105, 6807–6816, 2000.
- Bohren, G. F. and Huffman, D. R.: *Absorption and Scattering of Light by Small Particles*, John Wiley and Sons, 129–234, 1983.

Comparison of surface and column measurements of aerosol scattering

R. P. Aryal et al.

Title Page

Abstract

Introduction

Conclusions

References

Tables

Figures

⏪

⏩

◀

▶

Back

Close

Full Screen / Esc

Printer-friendly Version

Interactive Discussion

2007: The Physical Science Basis, Contribution of Working Group I to the Fourth Assessment Report of the Intergovernmental Panel on Climate Change, edited by: Solomon, S., Qin, D., Manning, M., Chen, Z., Marquis, M., Averyt, K. B., Tignor, M., and H. L. Miller, Cambridge University Press, Cambridge, UK and New York, NY, USA, 129–234, 2007.

5 Galloway, J. N., Keene, W. C., Artz, R. S., Church, T. M., and Knap, A. H.: Processes controlling the concentrations of SO_4^- , NO_3^- , NH_4^+ , H^+ , HCOO_T and CH_3COO_T in precipitation on Bermuda, *Tellus B*, 41, 427–443, 1989.

Galloway, J. N., Savoie, D. L., Keene, W. C., and Prospero, J. M.: The temporal and spatial variability of scavenging ratios for nss sulfate, nitrate, methane sulfonate and sodium in the atmosphere over the North Atlantic Ocean, *Atmos. Environ.*, 27, 235–250, 1993.

10 Holben, B. N., Eck, T. F., Slutsker, I., Tanreacute, D., Buis, J. P., Setzer, A., Vermote, E. F., Reagan, J. A., Kaufman, Y. J., Nakajima, T., Lavenu, F., Jankowiak, I., and Smirnov, A.: AERONET – a federated instrument network and data archive for aerosol characterization, *Remote Sens. Environ.*, 66, 1–16, 1998.

15 IPCC: Contribution of Working Group to the Fourth Assessment Report of the International Panel on Climate Change, Denarau Island, Nadi, Fiji, 20–22 June 2007, 2007.

Kaufman, Y. J., Gobbi, G. P., and Koren, I.: Aerosol climatology using a tunable spectral variability cloud screening of AERONET data, *J. Geophys. Res.*, 33, LO7817, doi:10.1029/2005GL025478, 2006.

20 Keene, W. C. and Savoie, D. L.: The pH of deliquesced sea-salt aerosol in polluted marine air, *Geophys. Res. Lett.*, 25, 2181–2184, 1998.

Keene, W. C. and Savoie, D. L.: Correction to “The pH of deliquesced sea-salt aerosol in polluted marine air”, *Geophys. Res. Lett.*, 26, 1315–1316, 1999.

Keene, W. C., Pszenny, A. P., Maben, J. R., and Sander, R.: Variation in marine aerosol acidity with particle size, *Geophys. Res. Lett.*, 29, 1101, doi:10.1029/2001GL013881, 2002.

25 King, M. D., Byrne, D. M., Herman, B. M., and Reagen, J. A.: Aerosol Size distributions obtained by inversion of spectral optical depths measurements, *J. Atmos. Sci.*, 35, 2153–2167, *Atmos. Environ.*, 30, 319–338, 1978.

Kleefeld, C., O’Dowd, C. D., O’Reilly, S., Jennings, S. G., Aalto, P., Becker, E., Kunz, G., and de Leeuw, G.: Relative contribution of submicron particles to aerosol light scattering in the marine boundary layer, *J. Geophys. Res.*, 107, 8103, doi:10.1029/2000JD000262, 2002.

30 Kokhanovsky, A. A.: *Aerosol Optics Light Absorption and Scattering by Particles in the Atmosphere*, Praxis Publishing, Chister, UK, 2008.

**Comparison of
surface and column
measurements of
aerosol scattering**

R. P. Aryal et al.

Title Page

Abstract

Introduction

Conclusions

References

Tables

Figures

◀

▶

◀

▶

Back

Close

Full Screen / Esc

Printer-friendly Version

Interactive Discussion

- Kotchenruther, R. A. and Hobbs, P. V.: Humidification factors of aerosols from biomass burning in Brazil, *J. Geophys. Res.*, 103, 32081–32089, 1998.
- Lawrence, M. G.: The relationship between relative humidity and the dew point temperature in moist air: a simple conversion and applications, *B. Am. Meteorol. Soc.*, 86, 225–233, 2005.
- 5 Lewis, E. R. and Schwartz, S. E.: *Sea Salt Aerosol Production: Mechanisms, Methods, Measurements and Models – a Critical Review*, American Geophysical Union, Washington, DC, 2004.
- Lewis, E. R. and Schwartz, S. E.: Comment on “Size distribution of sea-salt emissions as a function of relative humidity”, *Atmos. Environ.*, 40, 588–590, 2006.
- 10 Li, X., Maring, H., Savoie, D., Voss, K., and Prospero, J. M.: Dominance of mineral dust in aerosol light-scattering in the North Atlantic trade winds, *Nature*, 380, 416–419, 1996.
- Liu, B. Y. H., Pui, D. Y. H., and Wang, X. Q.: Sampling of carbon fiber aerosols, *Aerosol Sci. Tech.*, 2, 499–511, 1983.
- Moody, J. L., Oltmans, S. J., Levy II, H., and Merrill, J. T.: A transport climatology of tropospheric ozone, Bermuda: 1988–1991, *J. Geophys. Res.*, 100, 7179–7194, 1995.
- 15 Moody, J. L., Keene, W. C., Cooper, O. R., Voss, K. J., Aryal, R., Eckhardt, S., Holben, B., Maben, J. R., Izaguirre, M. A., and Galloway, J. N.: Flow climatology for physicochemical properties of dichotomous aerosol over the western North Atlantic Ocean at Bermuda, *Atmos. Chem. Phys. Discuss.*, 13, 22383–22444, doi:10.5194/acpd-13-22383-2013, 2013.
- 20 Reid, J. S., Hobbs, P. V., Ferek, R. J., Blake, D. R., Martins, J. V., Dunlap, M. R., and Liousse, C.: Physical, chemical, and optical properties of regional hazes dominated by smoke in Brazil, *J. Geophys. Res.*, 103, 32059–32080, 1998.
- Russel, P. B. and Heintzenberg, J.: An overview of the ACE2 clears sky column closure experiment (CLEAR COLUMN), *Tellus B*, 52, 463–483, 2000.
- 25 Savoie, D. L., Arimoto, R., Keene, W. C., Prospero, J. M., Duce, R. A., and Galloway, J. N.: Marine biogenic and anthropogenic contributions to non-sea-salt sulfate in the marine boundary layer over the North Atlantic Ocean, *J. Geophys. Res.*, 107, 4356, doi:10.1029/2001JD000970, 2002.
- Schuster, G. L., Dubovik, O., and Holben, B. N.: Angstrom exponent and bimodal aerosol size distributions, *J. Geophys. Res.*, 111, D07207, doi:10.1029/2005JD006328, 2006.
- 30 Sheridan, P. J., Delene, D. J., and Ogren, J. A.: Four years of continuous surface aerosol measurements from the Department of Energy’s Atmospheric Radiation Measurement Program

Comparison of surface and column measurements of aerosol scattering

R. P. Aryal et al.

Title Page

Abstract

Introduction

Conclusions

References

Tables

Figures

⏪

⏩

◀

▶

Back

Close

Full Screen / Esc

Printer-friendly Version

Interactive Discussion

Southern Great Plains Cloud and Radiation Test bed site 120, *J. Geophys. Res.*, 106, 20735–20747, 2001.

Seibert, P. and Frank, A.: Source-receptor matrix calculation with a Lagrangian particle dispersion model in backward mode, *Atmos. Chem. Phys.*, 4, 51–63, doi:10.5194/acp-4-51-2004, 2004.

Smirnov, A., Holben, B. N., Eck, T. F., Dubovik, O., Slutsker, I.: Cloud screening and quality control algorithms for the AERONET database, *Remote Sens. Environ.*, 73, 337–349, 2000.

Smirnov, A., Holben, B. N., Slutsker, I., Giles, D. M., McClain, C. R., Eck, T. F., Sakerin, S., M., Macke, A., Croot, P., Zibordi, G., Quinn, P. K., Sciare, J., Kinne, S., Harvey, M., Smyth, T. J., Piketh, S., Zielinski, T., Proshutinsky, A., Goes, J. I., Nelson, N. B., Larouche, P., Radionov, V. F., Goloub, P., Moorthy, K. K., Matarrese, R., Robertson, E. J., and Jourdin, F.: Maritime aerosol network as a component of aerosol robotic network, *J. Geophys. Res.*, 114, D06204, doi:10.1029/2008JD011257, 2009.

Spinhirne, J. D., Rall, J. A. R., and Scott, V. S.: Compact eye safe lidar systems, *Rev. Laser Eng. Laser Soc. Jpn.*, 23, 112–118, 1995.

Stohl, A., Hittenberger, M., and Wotawa, G.: Validation of the Lagrangian particle dispersion model FLEXPART against large scale tracer experiment data, *Atmos. Environ.*, 32, 4245–4264, 1998.

Stohl, A., Forster, C., Eckhardt, S., Spichtinger, N., Huntrieser, H., Heland, J., Schaller, H., Wilhelm, S., Arnold, F., and Cooper, O.: A backwater modeling study of inter-continental pollution transport using aircraft measurements, *J. Geophys. Res.*, 108, 4370, doi:10.1029/2002JD002862, 2003.

Stohl, A., Forster, C., Frank, A., Seibert, P., and Wotawa, G.: Technical note: The Lagrangian particle dispersion model FLEXPART version 6.2, *Atmos. Chem. Phys.*, 5, 2461–2474, doi:10.5194/acp-5-2461-2005, 2005.

Tang, I. N.: Thermodynamic and optical properties of mixed-salt aerosols of atmospheric importance, *J. Geophys. Res.*, 102, 1883–1893, 1997.

Turekian, V. C., Macko, S. A., and Keene, W. C.: Concentrations, isotopic compositions, and sources of size-resolved, particulate organic carbon and oxalate in near-surface marine air at Bermuda during spring, *J. Geophys. Res.*, 108, 4157, doi:10.1029/2002JD002053, 2003.

Voss, K. J., Welton, E. J., Quinn, P. K., Johnson, J. Thompson, A., and Gordon, H. R.: Lidar measurements during Aerosols 99, *J. Geophys. Res.*, 106, 20821–20832, 2001a.

**Comparison of
surface and column
measurements of
aerosol scattering**

R. P. Aryal et al.

Title Page

Abstract

Introduction

Conclusions

References

Tables

Figures

◀

▶

◀

▶

Back

Close

Full Screen / Esc

Printer-friendly Version

Interactive Discussion

Voss, K. J., Welton, E. J., Quinn, P. K., Frouin, R., Miller, M., and Reynolds, R. M.: Aerosol optical depth measurements during the Aerosols 99 experiment, *J. Geophys. Res.*, 106, 20811–20819, 2001b.

Wang, W., Rood, M. J., Carrico, C. M., Covert, D. S., Quinn, P. K., and Bates, T. S.: Aerosol optical properties along the north-east coast of North America during the New England Air Quality Study – Intercontinental Transport And Chemical Transformation 2004 campaign and the influence of aerosol composition, *J. Geophys. Res.*, 112, D10S23, doi:10.1029/2006JD007579, 2007.

Welton, E. J.: Measurements of Aerosol Optical Properties Over the Ocean Using Sun Photometry and Lidar, Ph.D. dissertation, Univ. of Miami, Coral Gables, FL., 1998.

Welton, E. J., Voss, K. J., Gordon, H. R., Maring, H., Smirnov, A., Holben, B. N., Schmidt, B., Livingston, J. M., Russell, P. B., Durkee, P. A., Formenti, P., and Andreae, M. O.: Ground based lidar measurements of aerosols during ACE-2: lidar description, results, and comparisons with other ground based and airborne measurements, *Tellus B*, 52, 636–651, 2000.

Welton, E. J., Campbell, J. R., Spinhirne, J. D., and Scott, V. S.: Global monitoring of clouds and aerosols using a network of micro-pulse lidar systems, in: *Lidar Remote Sensing for Industry and Environmental Monitoring*, edited by: Singh, U. N., Itabe, T., and Sugimoto, N., *Proc. SPIE*, 4153, 151–158, 2001.

Welton, E. J., Voss, K. J., Quinn, P. K., Flatau, P., Markowicz, K., Campbell, J. R., Spinhirne, J., Gordon, H. R., and J. E. Johnson, J. E.: Measurements of aerosol vertical profiles and optical properties during INDOEX 1999 using micropulse lidars, *J. Geophys. Res.*, 107, 8019, doi:10.1029/2000JD000038, 2002.

WMO/GAW Aerosol Measurement Procedures: Guidelines and Recommendations, TD No. 153, World Meteorological Organization/Global Atmosphere Watch, 2003.

Yan, P., Tang, J., Huang, J., Mao, J. T., Zhou, X.J., Liu, Q., Wang, Z. F., and Zhou, H. G.: The measurement of aerosol optical properties at a rural site in Northern China, *Atmos. Chem. Phys.*, 8, 2229–2242, doi:10.5194/acp-8-2229-2008, 2008.

Zieger, P., Weingartner, E., Henzing, J., Moerman, M., de Leeuw, G., Mikkilä, J., Ehn, M., Petäjä, T., Clémer, K., van Roozendaal, M., Yilmaz, S., Frieß, U., Irie, H., Wagner, T., Shaiganfar, R., Beirle, S., Apituley, A., Wilson, K., and Baltensperger, U.: Comparison of ambient aerosol extinction coefficients obtained from in-situ, MAX-DOAS and LIDAR measurements at Cabauw, *Atmos. Chem. Phys.*, 11, 2603–2624, doi:10.5194/acp-11-2603-2011, 2011.

Comparison of surface and column measurements of aerosol scattering

R. P. Aryal et al.

Table 1. Monthly average values of τ_{500} , $b_{\text{bulk-surf}}$, α and $R_{\text{sub-surf}}$ with standard deviation (σ). Number of hourly average data (N) used to get monthly average aerosol data are reported in parentheses in the second column.

| Months | $\tau_{500} \pm \sigma$ (N) | $b_{\text{bulk-surf}} \pm \sigma \text{ Mm}^{-1}$ | $\alpha \pm \sigma$ | $R_{\text{sub-surf}} \pm \sigma$ |
|--------|---------------------------------|---|---------------------|----------------------------------|
| Jan | 0.09 ± 0.02 (9) | 16.21 ± 4.01 | 0.77 ± 0.37 | 0.61 ± 0.19 |
| Feb | 0.09 ± 0.01 (6) | 6.96 ± 3.43 | 0.76 ± 0.16 | 0.53 ± 0.04 |
| Mar | 0.10 ± 0.01 (50) | 9.35 ± 3.94 | 0.94 ± 0.21 | 0.50 ± 0.13 |
| Apr | 0.14 ± 0.03 (56) | 17.23 ± 6.55 | 1.09 ± 0.29 | 0.70 ± 0.10 |
| May | 0.13 ± 0.03 (15) | 14.82 ± 4.41 | 0.59 ± 0.15 | 0.45 ± 0.07 |
| Jun | 0.15 ± 0.06 (6) | 12.84 ± 3.47 | 1.27 ± 0.11 | 0.67 ± 0.04 |

Title Page

Abstract

Introduction

Conclusions

References

Tables

Figures

⏪

⏩

◀

▶

Back

Close

Full Screen / Esc

Printer-friendly Version

Interactive Discussion

Comparison of surface and column measurements of aerosol scattering

R. P. Aryal et al.

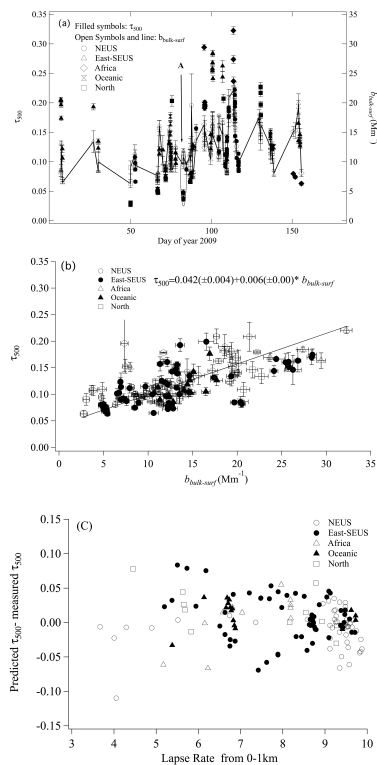


Fig. 1. (a) Time series column τ_{500} derived from CIMEL sun-photometer (AERONET products), and the corresponding $b_{\text{bulk-surf}}$ (b) scatter plot of these two parameters, and (c) lapse rate vs. τ_{500} predicted by $b_{\text{bulk-surf}}$. The line in (b) depicts a reduced major axis (RMA) regression (values in parentheses in the equation correspond to standard errors for the slope and intercept); the correlation coefficient is 0.65. Error bars depict standard deviation.

Comparison of surface and column measurements of aerosol scattering

R. P. Aryal et al.

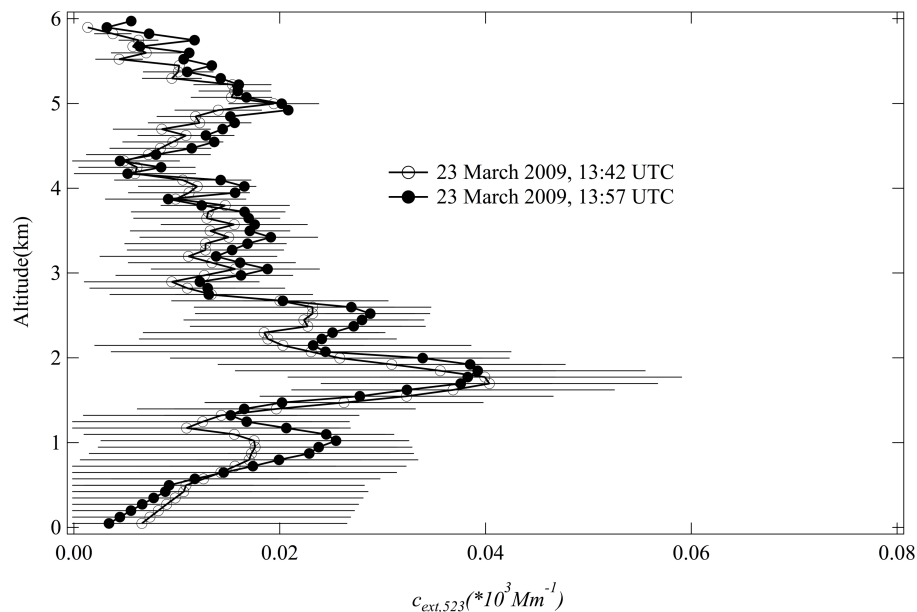


Fig. 2. Twenty-minute average MPL aerosol extinction profiles at 527 nm for two time periods on DOY 82. The error bars depict uncertainty of retrieval. τ_{500} during this period was 0.11.

[Title Page](#)[Abstract](#)[Introduction](#)[Conclusions](#)[References](#)[Tables](#)[Figures](#)[◀](#)[▶](#)[◀](#)[▶](#)[Back](#)[Close](#)[Full Screen / Esc](#)[Printer-friendly Version](#)[Interactive Discussion](#)

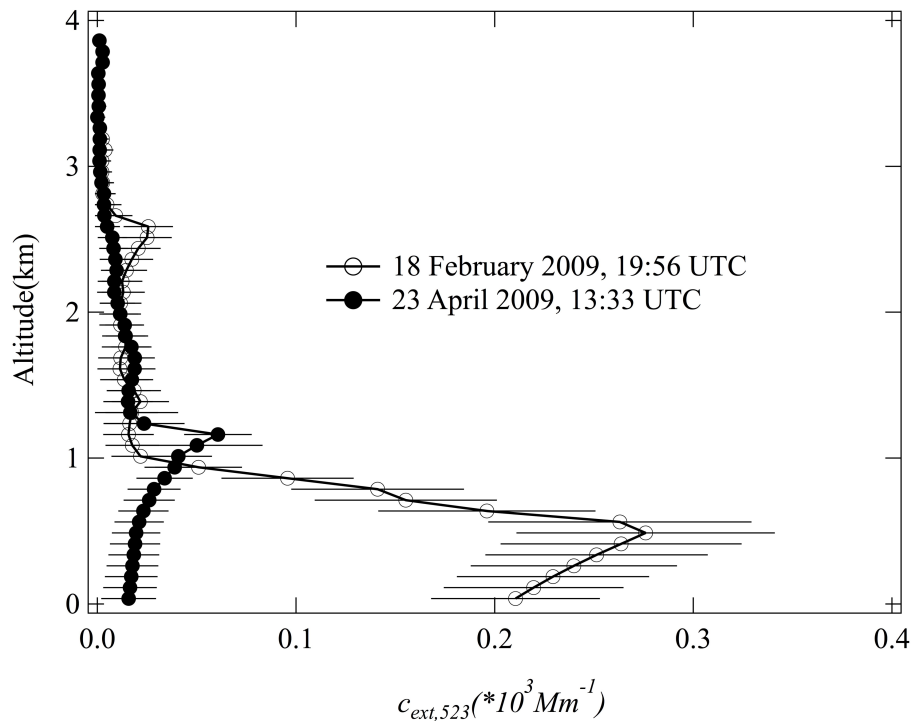


Fig. 3. Twenty-minute average vertical profiles of MPL aerosol extinction coefficients, $c_{\text{ext},527}$, at the time of the minima (18 February 2009) and maxima (23 April 2009) measurements of τ_{500} and $b_{\text{bulk-surf}}$. Error bars depict uncertainty for the retrieval.

Comparison of surface and column measurements of aerosol scattering

R. P. Aryal et al.

Title Page

Abstract Introduction

Conclusions References

Tables Figures

◀ ▶

◀ ▶

Back Close

Full Screen / Esc

Printer-friendly Version

Interactive Discussion



Comparison of surface and column measurements of aerosol scattering

R. P. Aryal et al.

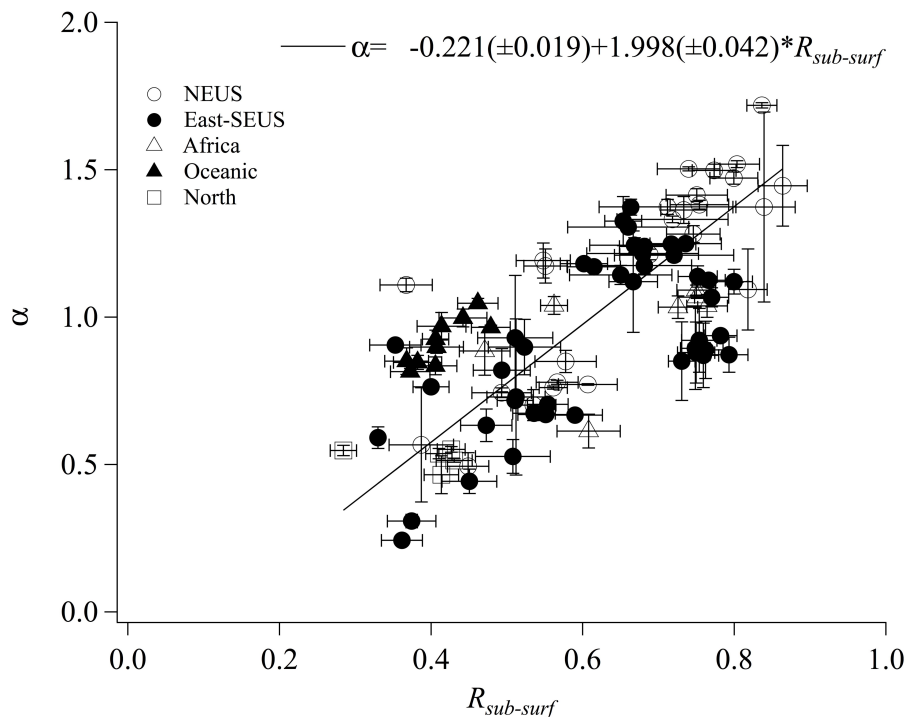


Fig. 4. Hourly averaged column α vs. hourly averaged $R_{sub-surf}$ for near-surface aerosol. The line depicts a RMA regression, values in parentheses in the equation correspond to standard errors, and the correlation coefficient is 0.72. Vertical and horizontal error bars depict standard deviation.

[Title Page](#)
[Abstract](#)
[Introduction](#)
[Conclusions](#)
[References](#)
[Tables](#)
[Figures](#)
[⏪](#)
[⏩](#)
[⏴](#)
[⏵](#)
[Back](#)
[Close](#)
[Full Screen / Esc](#)
[Printer-friendly Version](#)
[Interactive Discussion](#)

Comparison of surface and column measurements of aerosol scattering

R. P. Aryal et al.

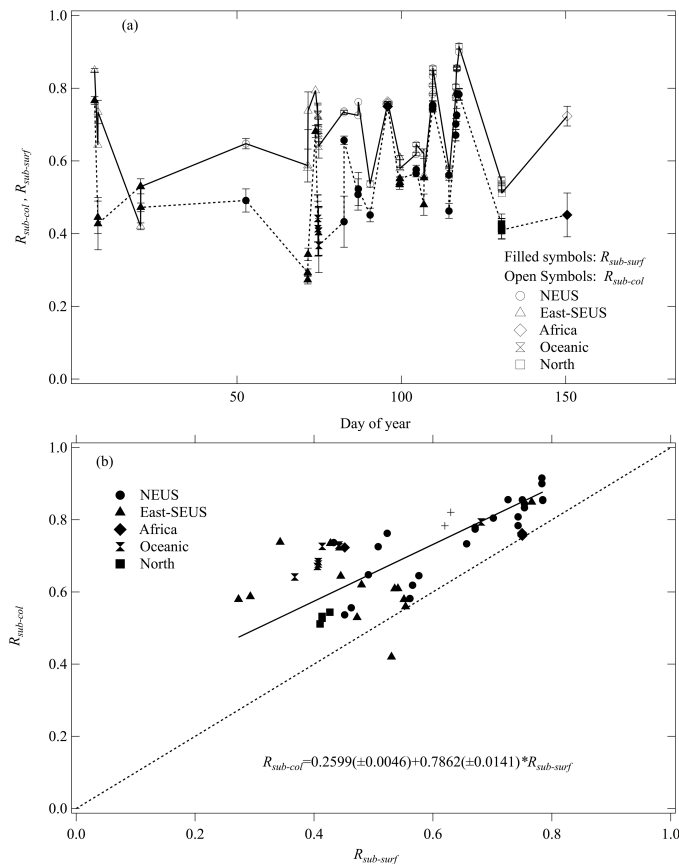


Fig. 5. (a) Time series column and near-surface sub- μm scattering fraction of light and (b) the corresponding scatter plot. The solid line depicts the RMA regression, values in parentheses correspond to standard errors, and the correlation coefficient is 0.76. The dashed line is the 1 : 1 line.

Comparison of surface and column measurements of aerosol scattering

R. P. Aryal et al.

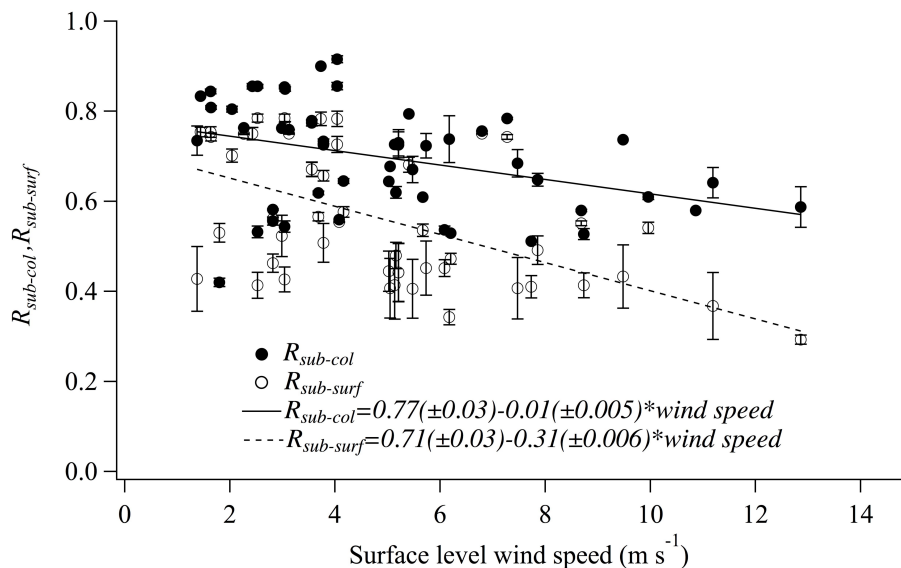


Fig. 6. Scatter plot of column and near-surface scattering fraction of light vs. wind speed. The corresponding correlation coefficients are 0.42 and 0.55, respectively. The lines depict RMA regressions for the indicated paired data.

[Title Page](#)
[Abstract](#)
[Introduction](#)
[Conclusions](#)
[References](#)
[Tables](#)
[Figures](#)
[Back](#)
[Close](#)
[Full Screen / Esc](#)
[Printer-friendly Version](#)
[Interactive Discussion](#)

Comparison of surface and column measurements of aerosol scattering

R. P. Aryal et al.

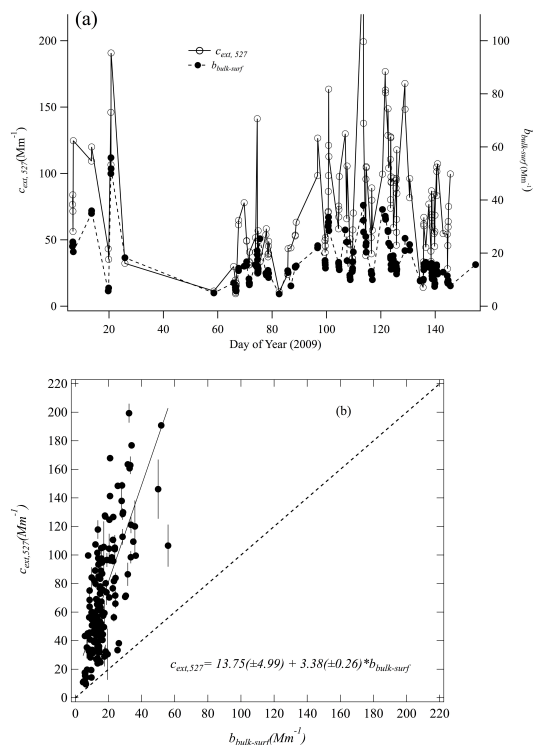


Fig. 7. Time series (a) and scatter plot (b) of the hourly averaged daytime extinction coefficient at the lowest height bin retrieved from the MPL data ($c_{\text{ext},527}$) vs. the scattering coefficient ($b_{\text{bulk-surf}}$). In (b) we show a RMA regression of the data and the 1 : 1 line. Values in parentheses in the equation are standard errors and the correlation coefficient is 0.71. Error bars depict standard deviation for the hourly averaged extinction coefficient, for scattering, this standard deviation is smaller than the symbol used for each data point.

Comparison of
surface and column
measurements of
aerosol scattering

R. P. Aryal et al.

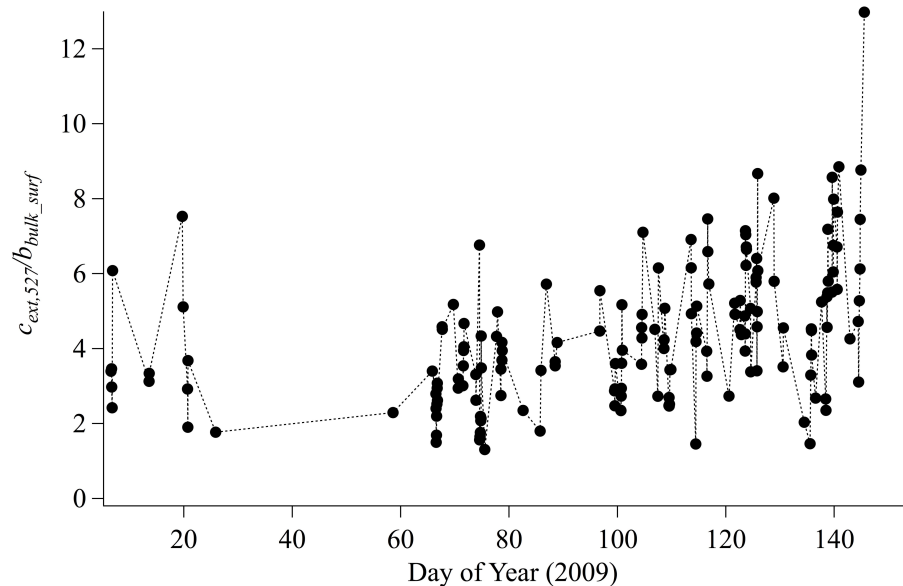


Fig. 8. Time series of $R_{mpl/neph}$.

[Title Page](#)[Abstract](#)[Introduction](#)[Conclusions](#)[References](#)[Tables](#)[Figures](#)[⏪](#)[⏩](#)[⏴](#)[⏵](#)[Back](#)[Close](#)[Full Screen / Esc](#)[Printer-friendly Version](#)[Interactive Discussion](#)

Comparison of surface and column measurements of aerosol scattering

R. P. Aryal et al.

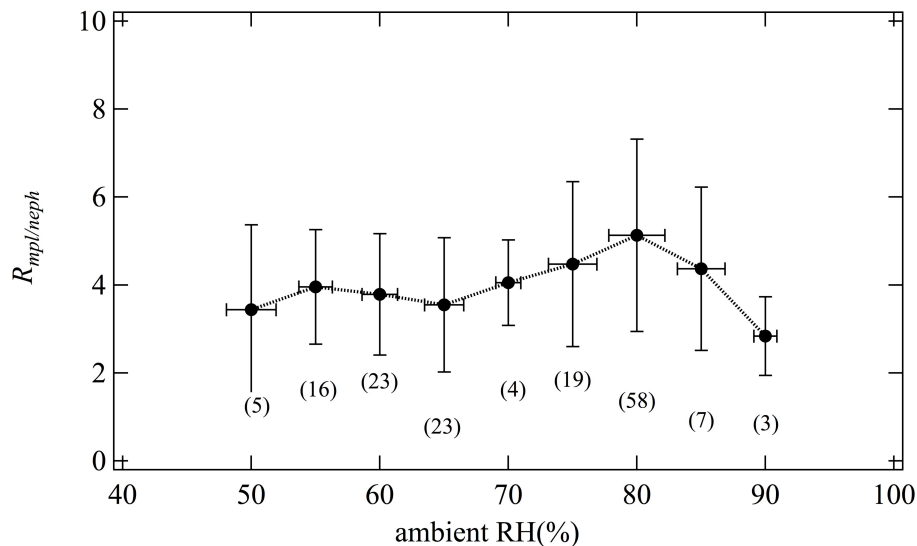


Fig. 9. Averages and standard deviations for $R_{mpl/neph}$ over 5% RH bins vs. ambient RH (%).

[Title Page](#)[Abstract](#)[Introduction](#)[Conclusions](#)[References](#)[Tables](#)[Figures](#)[⏪](#)[⏩](#)[⏴](#)[⏵](#)[Back](#)[Close](#)[Full Screen / Esc](#)[Printer-friendly Version](#)[Interactive Discussion](#)